

# UC Santa Barbara

## UC Santa Barbara Previously Published Works

### Title

Carbon doping of GaN with CBr<sub>4</sub> in radio-frequency plasma-assisted molecular beam epitaxy

### Permalink

<https://escholarship.org/uc/item/05k946ng>

### Journal

Journal of Applied Physics, 95(12)

### ISSN

0021-8979

### Authors

Green, D S  
Mishra, U K  
Speck, J S

### Publication Date

2004-06-01

Peer reviewed

# Carbon doping of GaN with $\text{CBr}_4$ in radio-frequency plasma-assisted molecular beam epitaxy

D. S. Green and U. K. Mishra

*Electrical and Computer Engineering Department, University of California, Santa Barbara, California 93106*

J. S. Speck<sup>a)</sup>

*Materials Department, University of California, Santa Barbara, California 93106*

(Received 11 November 2003; accepted 5 April 2004)

Carbon tetrabromide ( $\text{CBr}_4$ ) was studied as an intentional dopant during rf plasma molecular beam epitaxy of GaN. Secondary ion mass spectroscopy was used to quantify incorporation behavior. Carbon was found to readily incorporate under Ga-rich and N-rich growth conditions with no detectable bromine incorporation. The carbon incorporation  $[\text{C}]$  was found to be linearly related to the incident  $\text{CBr}_4$  flux. Reflection high-energy electron diffraction, atomic force microscopy and x-ray diffraction were used to characterize the structural quality of the film's postgrowth. No deterioration of structural quality was observed for  $[\text{C}]$  from mid  $10^{17}$  to  $\sim 10^{19} \text{ cm}^{-3}$ . The growth rate was also unaffected by carbon doping with  $\text{CBr}_4$ . The electrical and optical behavior of carbon doping was studied by co-doping carbon with silicon. Carbon was found to compensate the silicon although an exact compensation factor was difficult to extract from the data. Photoluminescence was performed to examine the optical performance of the films. Carbon doping was seen to monotonically decrease the band edge emission. Properties of carbon-doped GaN are interpreted to be consistent with recent theoretical work describing incorporation of carbon as function of Fermi level conditions during growth. © 2004 American Institute of Physics. [DOI: 10.1063/1.1755431]

## I. INTRODUCTION

The role of carbon in GaN has been discussed extensively because of its prevalence as an unintentional impurity (along with hydrogen and oxygen) as well as its potential utility as an intentional dopant. Despite significant theoretical and experimental work, there is no clear consensus as to the nature of the carbon impurity. This is largely a result of the difficulty in independently controlling carbon incorporation when growing GaN films.

Initially, the role of carbon in GaN was investigated primarily as it related to photoluminescence (PL) properties of films containing carbon. Many of these studies focused on the yellow luminescence (YL) peak roughly centered around 2.2 eV, and were motivated by two early studies. Pankove and Hutchby's early studies of ion implanted GaN first remarked upon the YL peak.<sup>1</sup> In these studies, samples with several different implant species exhibited broad luminescence centered around 2.2 eV, hence no correlation was made between the YL peak and the carbon impurity. Rather, they attributed the YL peak to damage caused in the GaN by the ion implantation process. However, the early material used by Pankove and Hutchby likely had a high concentration of unintentional impurities, including carbon, which could have been associated with the YL peak. Ogino and Aoki first attributed the yellow luminescence (YL) prevalent in their GaN film to a transition involving carbon.<sup>2</sup> Their study correlated the carbon impurity level in GaN microcrys-

tals and needle-like films synthesized by direct reaction of  $\text{NH}_3$  and gallium to temperature dependent shifts in intensity and peak position of YL and band edge PL peaks. From these thermal quenching experiments, they extracted a carbon acceptor energy level to be 860 meV above the valence band maximum. To this acceptor level, the YL centered around 2.2 eV was correlated to a phonon-assisted transition from a shallow donor. In this experiment the carbon concentration was controlled by changing the boat containing the samples as they were grown, again indicating an early difficulty in controlling unintentional impurities.

With the advent of more mature growth technologies for GaN, the number of explanations for YL have increased dramatically. The correlation of carbon concentration and YL intensity was widely reported,<sup>3,4</sup> but the microscopic mechanism for the YL was not clearly elucidated. Glaser *et al.* and Hofmann *et al.* reported measurements on optically detected magnetic resonance that indicated the YL transition involved a deep donor, with carbon suggested to be a shallow acceptor.<sup>5,6</sup> The deep donor in these studies was speculated to be a deep double donor due to nitrogen vacancies, though no deep donor level has been verified to date. Similarly, Fischer *et al.* attributed an acceptor site of 230 meV depth to carbon impurities based on thermal quenching experiments on near band edge PL peaks.<sup>7</sup> However, Perlin *et al.* reported that the YL transition was more likely due to deep acceptor levels, though not necessarily carbon related.<sup>8,9</sup> The discrepancy between the two explanations was addressed by Polyakov *et al.* who discussed the likelihood of two overlapping bands responsible for the YL in the context of PL measurements on AlGaIn samples of varying composition.<sup>10</sup> Zhang

<sup>a)</sup> Author to whom correspondence should be addressed; electronic mail: speck@mrl.ucsb.edu

and Kuech then correlated YL to carbon concentration by intentionally doping halide vapor phase epitaxy (HVPE) grown GaN with propane.<sup>11</sup> Their results also indicate two overlapping YL bands with the carbon doping corresponding to an increase in intensity and shift in peak energy of the YL peak. However, they assigned no energetic position to the carbon impurity. Other groups have also associated carbon with at least one mechanism for YL, though the role of native defects and other impurities remains unclear.<sup>12,13</sup>

Concurrent to the experimental work investigating the role of carbon, theoretical efforts have focused on the role of carbon and other native defects potentially occupying deep levels. The first studies looked at carbon as a substitutional impurity, with interstitial incorporation thought to be unlikely. While an initial study suggested that carbon substituting for N ( $C_N$ ) was a deep acceptor,<sup>14</sup> other groups calculated that  $C_N$  was likely to be a shallow acceptor.<sup>15,16</sup> More recently, work by Wright indicates that beyond the  $C_N$  site, which he found to be a shallow acceptor, and carbon substituting for Ga ( $C_{Ga}$ ), a shallow donor, carbon interstitial ( $C_I$ ) sites and  $C_I-C_N$  complexes with transitions near 2.1 eV can have favorable formation energetics depending on the Fermi level during growth.<sup>17</sup> Essentially, Wright found that the growth conditions and Fermi level position favor self-compensation. Thus  $C_N$  is likely to be incorporated for  $n$ -type material, while  $C_{Ga}$ ,  $C_I$  and the  $C_I-C_N$  complex is likely to form in  $p$ -type material with the relative concentrations depending upon the growth stoichiometry. The understanding of the carbon impurity has evolved in parallel to the development in the understanding of native defects in GaN. The nitrogen vacancy,  $V_N$ , has generally been attributed to be a shallow donor.<sup>18</sup> The gallium vacancy,  $V_{Ga}$ , was initially calculated to be a shallow acceptor,<sup>19,20</sup> though it is also found to be a deep acceptor when complexed with other impurities.<sup>15</sup> Recent calculations, however, suggest that  $V_{Ga}$  is a deep acceptor in noncomplexed configuration as well.<sup>17</sup> In summary, theoretical studies suggest the best candidates for the 2.2 eV PL transition are  $V_{Ga}$  as well as  $C_{Ga}$  under Ga-rich growth conditions and  $C_I$  and  $C_I-C_N$  complexes under N-rich growth conditions.<sup>21</sup> Thus, while the role of carbon can be potentially explained by theories, the presence of competing mechanisms still leaves the exact nature of carbon incorporation in doubt.

Several groups have tried to resolve this convolution of carbon behavior with other impurity behavior by looking at films with intentional carbon doping and using a variety of electrical and optical characterization techniques. In each case, it is difficult to separate the subsequent behavior of the material as being coincidental or causally related to carbon. Studies using metalorganic chemical vapor deposition (MOCVD) are limited in addressing this problem because the presence of the metalorganics makes unintentional carbon incorporation ubiquitous, though at low levels. Further, to controllably incorporate greater concentrations of carbon, the growth pressure is generally lowered and thus potentially changing the native defect level in addition to changing the carbon impurity level or concentration.<sup>22</sup> Despite these shortcomings, experimental results from Seager *et al.* strongly suggest that carbon in MOCVD growth will incorporate as a

shallow acceptor when the Fermi level is near the conduction band and will tend to self-compensate otherwise.<sup>21</sup> This explanation is also consistent with the experimental evidence that films grown at low pressure show deep levels and one of these deep levels associated with carbon has been found to cause current collapse in field effect transistor structures.<sup>23</sup> Yet, without a truly independent method to vary carbon concentration, experiments with MOCVD material will not be definitive. HVPE films, generally grown with nominally carbon-free sources, are limited by the impurities present in the source gases, particularly  $NH_3$ .

Molecular beam epitaxy (MBE) growth of GaN provides the potential to controllably incorporate carbon in GaN independently from other growth parameters. To date, several groups have tried this approach with carbon sources including  $CCl_4$ , methane cracked in plasma, and electron beam evaporated graphite. However, in each case the carbon source introduces alternative problems with the carbon doping mitigating the advantage of the purity inherent to the MBE method. Using  $CCl_4$  as a carbon source, groups have demonstrated compensation of  $n$ -type material and  $p$ -type material in cubic GaN on GaAs.<sup>24-26</sup> However, two factors complicate these measurements: the carbon source was found to etch the material during growth reducing the growth rate, potentially increasing incorporation of other unintentional dopants responsible for  $p$ -type conductivity, and the unintentional carrier concentration is typically  $p$  type in cubic GaN on GaAs. The use of heated graphite appeared to demonstrate that carbon incorporation could compensate  $n$ -type films but the carbon source did not appear well controlled.<sup>27</sup> Finally, the use of methane with a plasma cracking source has demonstrated semi-insulating (SI) films with controlled carbon incorporation, but the x-ray rocking curve linewidths almost doubled in the carbon doped material, suggesting a deterioration in material quality may also be responsible for the semi-insulating nature of the films.<sup>28</sup>

$CBr_4$  is well established for use as a shallow acceptor in other III-V materials. While there has been a single report on the intentional doping of GaN by  $CBr_4$ ,<sup>29</sup> there has been no comprehensive study detailing its behavior as a dopant in GaN. This work looks at the use of  $CBr_4$  to provide an efficient source for carbon doping in GaN. Carbon doped films were then examined to study the optical and electronic properties of GaN:C.

## II. EXPERIMENT

All GaN films were grown in a Varian Modular Gen II system. The active nitrogen was supplied by an EPI Unibulb rf plasma nitrogen source. Conventional effusion cells were used for gallium and silicon. All samples were grown on templates of MOCVD-grown GaN (0001) on sapphire. The GaN templates were either  $n$ -type GaN  $\sim 2 \mu m$  thick with silicon concentrations  $[Si]$  of  $\sim 10^{18} cm^{-3}$  or semi-insulating (SI) GaN  $\sim 2 \mu m$  thick doped with a subsurface Fe layer as described elsewhere.<sup>30</sup> All samples were grown with a rf power of 150 W and a sufficient  $N_2$  flow to maintain a chamber pressure of  $1.1 \times 10^{-5}$  Torr. These conditions correspond to a growth rate of  $\sim 200$  nm/h or  $\sim 0.2$  ML/s. The carbon

TABLE I. Summary of sample growth conditions and structures where varied quantities are labeled I.V. and D.V. to indicate independent and dependent variables, respectively.

Sample	Template	III/V ratio	$T_{\text{growth}}$ °C	$P_{\text{foreline}}$ mTorr	[C] $10^{18} \text{ cm}^{-3}$	[Si] $10^{18} \text{ cm}^{-3}$	$n_{\text{Hall}}$ $10^{18} \text{ cm}^{-3}$	Structure
A1	GaN:Si	Ga rich	I.V.	10	D.V.			Doping calibration
A2	GaN:Si	N rich	I.V.	10	D.V.			Doping calibration
A3	GaN:Si	Ga rich	650	I.V.	I.V.			Doping calibration
A4	GaN:Si	Ga rich	I.V.	10	D.V.			Doping calibration
A5	GaN:Si	Ga rich	650					90 nm GaN/10 nm AlGaIn
A6	GaN:Si	Ga rich	650	20	10			90 nm GaN:C/10 nm AlGaIn
B1	SI GaN	Ga rich	650	0		1	1	$\sim 0.45 \mu\text{m}$ GaN:Si+C
B2	SI GaN	Ga rich	650	1	0.9	1	0.17	$\sim 0.45 \mu\text{m}$ GaN:Si+C
B3	SI GaN	Ga rich	650	5	2.9	1	Res.	$\sim 0.45 \mu\text{m}$ GaN:Si+C
B4	SI GaN	Ga rich	650	10	5.4	1	Res.	$\sim 0.45 \mu\text{m}$ GaN:Si+C
B5	SI GaN	Ga rich	650	20	10	1	Res.	$\sim 0.45 \mu\text{m}$ GaN:Si+C
C1	SI GaN	Ga rich	650	N/A	N/A	7	6.9	$\sim 0.45 \mu\text{m}$ GaN:Si+C
C2	SI GaN	Ga rich	650	2.5	1.7	7	4.4	$\sim 0.45 \mu\text{m}$ GaN:Si+C
C3	SI GaN	Ga rich	650	7.5	4.2	7	5.0	$\sim 0.45 \mu\text{m}$ GaN:Si+C

source was a commercially available carbon tetrabromide ( $\text{CBr}_4$ ) sublimation system. The system used an automated control valve to throttle the vapor pressure from the solid source at room temperature to a foreline, thus the control variable  $P_{\text{foreline}}$  was used to control the  $\text{CBr}_4$  flow. Finally, the gas then passed from the foreline through a leak valve, reducing the pressure, and was introduced into the growth chamber.

Reflection high-energy electron diffraction patterns were recorded *in situ* prior to and postgrowth at growth temperature and upon cooling to a substrate temperature of less than  $\sim 250^\circ\text{C}$ . Postgrowth, the gallium surface coverage was monitored by optical microscopy. The Ga-rich samples were observed to have gallium droplets postgrowth, while the N-rich samples were not observed to have any droplets. Subsequently, the samples were etched in HCl to remove excess gallium and the surface morphology was imaged by atomic force microscopy (AFM). Secondary ion mass spectroscopy (SIMS) performed on a Physical Electronics 6650 quadrupole dynamic secondary ion mass spectrometer was used to establish the carbon, oxygen, bromine, and silicon concentrations. Photoluminescence (PL) measurements were performed using the 325 nm line from a HeCd laser with an excitation density of  $\sim 400 \text{ kW/cm}^2$ . High resolution x-ray diffraction (XRD) measurements were performed using a Philips Materials Research Diffractometer. Hall measurements were taken in the Van der Pauw geometry using In dots as ohmic contacts.

Three sample series were grown. The first set of samples, series A, was grown to determine carbon incorporation and establish baseline carbon concentrations for subsequent experiments. To this end, six samples were grown. Samples A1 and A2 were grown to establish the carbon flux for three substrate temperatures for Ga-rich and N-rich growth conditions. Sample A2 was the only sample grown under N-rich growth conditions. For both samples, A1 and A2, the growth began with a 15 min buffer, then three 30 min GaN:C layers were grown separated by 15 min spacer layers during which the temperature was changed and stabilized. The substrate temperatures used were 600, 650, and  $700^\circ\text{C}$ .

Sample A3 was grown to determine carbon incorporation for varying incident  $\text{CBr}_4$  flux for a given substrate temperature of  $650^\circ\text{C}$  under Ga-rich grown conditions. Sample A4 was grown for a carbon flux under Ga-rich growth conditions, with varying substrate temperature. In sample A4,  $\sim 90 \text{ nm}$  GaN:C was grown at five substrate temperatures of 600, 625, 650, 675, and  $700^\circ\text{C}$ , separated by  $\sim 90 \text{ nm}$  of unintentionally doped GaN during which the substrate temperature was changed and stabilized. Finally, samples A5 and A6 consisted of  $\sim 90 \text{ nm}$  of GaN, doped and un-doped with carbon respectively, on a thin AlGaIn layer to determine any change in the growth rate of the material.

The second and third sample series were designed to look at the structural, electrical, and optical properties for varying doping levels of carbon with a constant background level of intentionally doped silicon. Five samples were grown in series B with a varying flux of carbon for a constant silicon background of  $\sim 10^{18} \text{ cm}^{-3}$ . Three samples were grown in series C with a constant silicon background of  $\sim 7 \times 10^{18} \text{ cm}^{-3}$ . All samples from series B and C were grown on SI GaN templates and consisted of  $\sim 0.45 \mu\text{m}$  GaN co-doped with silicon and carbon. The doping levels and a summary of all growth conditions can be found in Table I.

### III. RESULTS

The first experiment investigating the incorporation of carbon from the  $\text{CBr}_4$  source showed promising doping behavior. SIMS measurements, shown in Fig. 1, on sample A1 grown under Ga-rich conditions demonstrate the ready incorporation of carbon with measured carbon concentrations [C] as high as mid- $10^{19} \text{ cm}^{-3}$ . The bromine concentration was at the SIMS detection limit of  $\sim 10^{15} \text{ cm}^{-3}$ . Additionally, the oxygen level did not appear to increase beyond the low unintentional impurity level typical of our films (mid- $10^{16} \text{ cm}^{-3}$ ). Note that a spike for all impurities was observed at the MOCVD/MBE regrowth interface, however it is unclear whether this is a result of impurity gettering during growth or simply contamination of the surface prior to regrowth. The increase of the substrate temperature resulted in

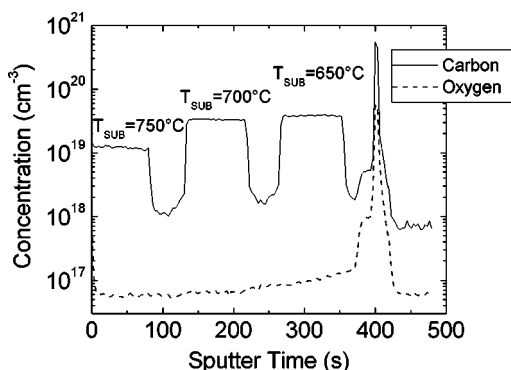


FIG. 1. SIMS measurement from sample A1 grown under Ga-rich conditions for substrate temperatures 600, 650, and 700 °C showing an abrupt carbon doping profile and decreasing incorporation for increasing substrate temperature.

a decrease in the level of carbon incorporation, this was investigated more in sample A4 discussed below. Sample A2, grown under N-rich conditions, shows similar results to sample A1 as can be seen in Fig. 2. The decrease in doping profile abruptness for the A2 can be partially attributed to the increased surface roughness associated with N-rich growth conditions. The oxygen level in A2 was higher than A1 throughout (typical for N-rich growth conditions) and particularly increased during the layers doped with carbon. The reasons for this increase are unclear and will be discussed below. Finally, the level of carbon incorporation was comparable for the Ga-rich and N-rich growth conditions after correcting for the difference in growth rate.

The rest of series A investigated the dependence of carbon incorporation on CBr<sub>4</sub> flux and substrate temperature and the impact of CBr<sub>4</sub> flux on growth rate. Sample A3 was grown to determine carbon incorporation as function of incident CBr<sub>4</sub> flux. The SIMS measurements on sample A3 [Fig. 3(a)] revealed abrupt junction profiles with interfaces of ~8 nm/dec. Additionally, the carbon concentration in the GaN had a linear dependence on the incident CBr<sub>4</sub> flux as shown in Fig. 3(b). The carbon source is thus demonstrated to be linear and provide abrupt doping profiles. SIMS measurements of sample A4, shown in Fig. 4, demonstrate that the

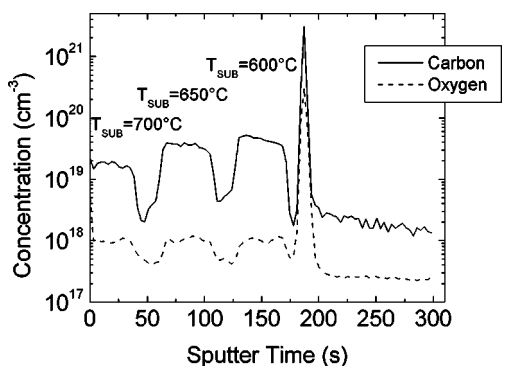


FIG. 2. SIMS measurement from sample A2 grown under N-rich conditions for substrate temperatures 600, 650, and 700 °C showing a rounded carbon doping profile, likely due to surface roughness, and decreasing incorporation for increasing substrate temperature. Oxygen incorporation was also seen to rise in regions of carbon doping.

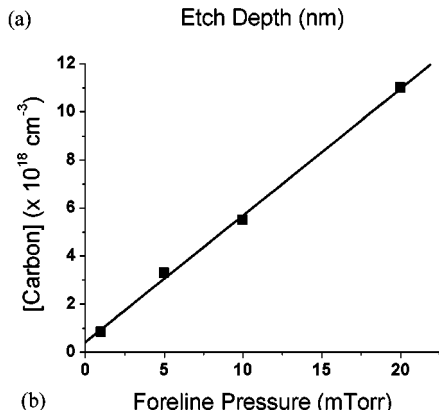
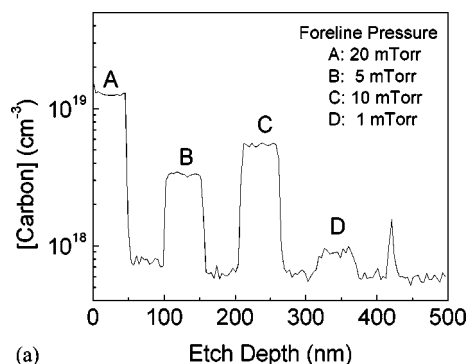


FIG. 3. Sample A3 SIMS measurement showing (a) the carbon concentration changing as a function of the incident CBr<sub>4</sub> flux and (b) the linear relationship between carbon concentration and incident flux.

carbon incorporation is sensitive to the substrate temperature. Increasing the substrate temperature led to a decrease in carbon incorporation. Plots of ln [C] vs 1/kT were not linear thus no meaningful activation energy to the process could be extracted. This result potentially indicates that more than one process is responsible for the decrease in carbon incorporation. Samples A5 and A6 were used to establish the impact of carbon doping on the growth rate. The structure of each sample was a GaN layer on top of a thin AlGaN spacer layer. Interference patterns in ω-2θ XRD scans of the (0002) diffraction peak, seen in Fig. 5, exhibited a periodicity that is sensitive only to the thickness of the top GaN layer. Thus an extremely accurate measure of the growth rate was made. The growth rate difference between heavily carbon doped and undoped samples was negligible.

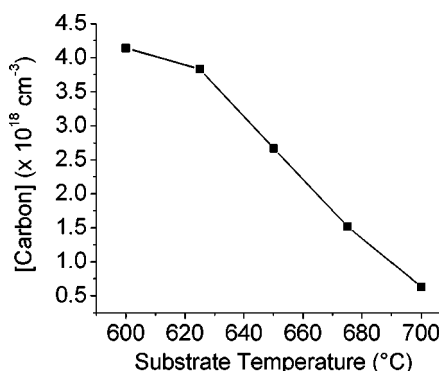


FIG. 4. Temperature dependence of carbon incorporation as measured by SIMS in sample A4 showing the decrease in carbon doping with increase in substrate temperature.

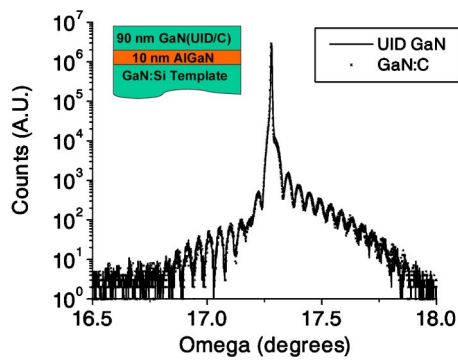


FIG. 5. A  $\omega$ - $2\theta$  x-ray diffraction scan of (0002) diffraction peak showing the negligible impact of carbon doping on growth rate.

The series B and C samples were designed to study the impact of carbon when co-doped with silicon on structural, optical, and electrical properties. XRD rocking curve scans of the series B samples revealed no change in the (0002) and the (10 $\bar{1}2$ ) peak widths. The rocking curve linewidths for these samples were all in the range 265–280 arcsec<sup>-1</sup> around the (0002) peak and in the range 625–750 arcsec<sup>-1</sup> around the (1012) peak as the carbon concentration changed from  $\sim 10^{16}$  to  $\sim 10^{19}$  cm<sup>-3</sup>. Thus, no deterioration in structural quality is associated with carbon doping. This is supported by the AFM scans which show surface morphology typical of Ga-rich MBE growth. A scan of sample C2 can be seen in Fig. 6 and is typical of all samples grown under Ga-rich conditions. The morphology has a rms roughness of  $\sim 8$  nm and indicates spiral, step flow growth mediated by mixed character dislocations. Thus no impact of carbon is seen on the structural or morphological properties of the films.

The optical and electrical properties show a more varied impact of the carbon doping. Hall measurements on the co-doped samples showed a reduction in carrier concentration as the carbon doping was increased, as shown in Fig. 7. The compensation factor was almost unity for series B. However, the numerical results from series C did not indicate a single compensation factor. The reason for this discrepancy is likely

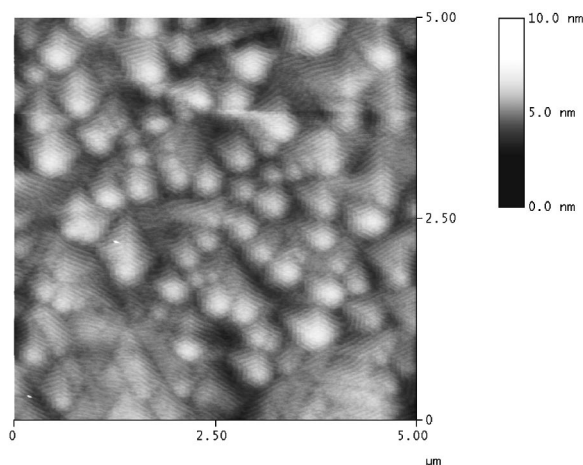


FIG. 6. AFM scan from sample C2 showing a representative GaN:C surface morphology under Ga-rich growth conditions with a rms roughness of  $\sim 8$  nm.

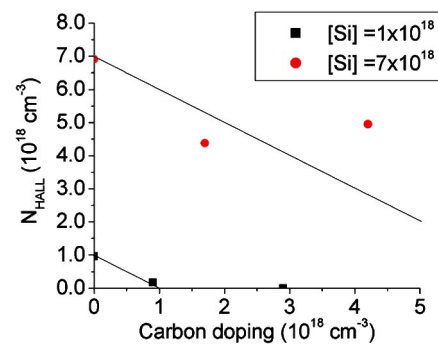


FIG. 7. Hall results from series B and C showing compensation of the  $n$ -type carrier concentration with the increase in carbon doping.

due to the unintentional donors found at the regrowth interface. The MBE regrowth interface is known to contain a large number of impurities and likely serves as a leakage pathway. This suspicion was confirmed by progressively dry etching a sample and incrementally measuring the conductance between two contacts. The conductance remained relatively constant before dropping abruptly upon etching through the regrowth interface. Thus, the electrical measurements reported here accurately indicate that the carbon will compensate the silicon donors but the numerical evaluation of the carbon efficiency is compromised by the leakage path. Additionally, the presence of charge at the regrowth interface has been confirmed by capacitance–voltage measurements on other carbon-doped samples not reported on here.

PL measurements of the series B samples yielded a number of interesting observations. The raw spectrum from these measurements can be seen in Fig. 8(a). Peaks were observed in the spectrum centered at the energies: 1.7, 2.2, 2.85, and 3.4 eV. The integrated peak intensities were calculated by fitting multiple Gaussian peaks to the spectra and are shown in Fig. 8(b) for different carbon doping concentrations. The first observation from the spectra is the monotonic attenuation of the band edge luminescence with increasing carbon doping. Additionally a peak at 1.7 eV was observed and was attenuated for increasing carbon concentration. The reduction of the 1.7 eV peak below the detection limit corresponds to the compensation of the  $n$ -type carrier concentration measured via Hall. Finally, the introduction of carbon corresponds to the introduction of the PL peaks at 2.2 and 2.85 eV. These peaks have a maximum intensity for a carbon concentration of  $2.9 \times 10^{18}$ . Our ongoing PL studies are focused on the relative intensity of the deep levels with varying pump power.

#### IV. DISCUSSION

The incorporation of carbon is seen from the SIMS measurements to be linear with incident  $\text{CBr}_4$  flux and dependent on substrate temperature. Additionally, sample A2 showed the oxygen level followed the carbon incorporation level. The reason for this can be explained by Fermi level considerations. Incorporation of  $\text{C}_\text{N}$  would introduce an acceptor in the crystal and the resultant movement of the Fermi level toward the valence band would make the incorporation of oxygen, a shallow donor, more likely. An alternate explana-

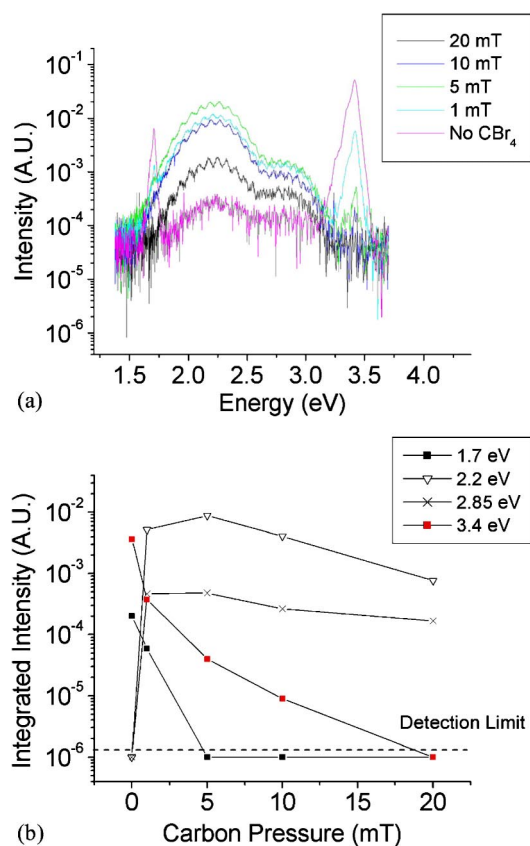


FIG. 8. GaN:C PL showing the (a) raw scans of the PL spectrum and (b) the integrated intensity of the various PL peaks as a function of carbon doping.

tion would be that the CBr<sub>4</sub> source contains oxygen as an impurity in the source which is introduced at the same time as the carbon. Yet the absence of this increase in oxygen for the Ga-rich growth conditions suggests the source is not likely the source of the difference. However, the gallium bilayer on the surface may serve to reduce any additional oxygen from the source as it reduces the unintentionally incorporated oxygen in the nonintentionally doped GaN.<sup>31</sup>

The electrical measurements on series B and C clearly demonstrate the compensating nature of the carbon doping for *n*-type films. However, no *p*-type conduction was measured on these samples or on samples grown without silicon co-doping under similar conditions. This indicates that carbon will also self-compensate when it is the primary dopant. Additional experiments on completely MBE grown material, eliminating the regrowth interface difficulty, and in *p*-type material are needed to clarify the exact compensation factor for the carbon, preliminarily suggested to be unity here. However, the compensating behavior suggests carbon doping with CBr<sub>4</sub> will be useful for growth of semi-insulating buffers in transistor structures.

The band edge peak intensity from the PL decreased with increasing carbon concentration and may be interpreted to result from a loss of free electrons to compensating acceptors. PL measurements support the correlation of carbon with the 2.2 eV PL peak as well as the 2.85 eV peak. The dependence of peak intensity, however, appeared to be a complicated balance of the increase in the states involved in the

transition against the decrease in free electrons and increase of nonradiative states.

## V. CONCLUSION

CBr<sub>4</sub> has been shown to be an effective source of carbon for GaN films grown by rf plasma MBE. Carbon incorporation has been shown to be linear with incident flux and to have an abrupt doping profile. The CBr<sub>4</sub> has negligible impact on the GaN growth rate, growth mode, and structure. The temperature dependence of carbon incorporation does not show a simple Arrhenius dependence but does show decreased incorporation for increasing growth temperatures. The electrical and optical impact of carbon doping has been found to be consistent with recent theoretical work which indicates carbon incorporation to be related to the growth conditions and Fermi level during growth. Generally, the carbon seeks to self-compensate during growth, decreasing carrier concentration and reducing band edge luminescence in *n*-type samples co-doped with silicon.

## ACKNOWLEDGMENTS

The authors would like to acknowledge Tom Mates for help with the SIMS measurements as well as Patrick Walterit, Sten Heikman, and Stacia Keller for discussions related to the PL of GaN. This work was supported by AFOSR (G. Witt, contract monitor). Additionally, D.G. was supported by a NSF Graduate Research Fellowship.

- <sup>1</sup>J. I. Pankove and J. A. Hutchby, *J. Appl. Phys.* **47**, 5387 (1976).
- <sup>2</sup>T. Ogino and M. Aoki, *Jpn. J. Appl. Phys., Part 1* **19**, 2395 (1980).
- <sup>3</sup>A. Ishibashi, H. Takeishi, M. Mannoh, Y. Yabuuchi, and Y. Ban, *J. Electron. Mater.* **25**, 799 (1996).
- <sup>4</sup>R. Niebuhr, K. Bachem, K. Dombrowski, M. Maier, W. Pletschen, and U. Kaufmann, *J. Electron. Mater.* **24**, 1531 (1995).
- <sup>5</sup>E. R. Glaser, T. A. Kennedy, K. Doverspike, L. B. Rowland, D. K. Gaskill, J. A. Freitas, Jr., M. Asif Khan, D. T. Olson, J. N. Kuznia, and D. K. Wickenden, *Phys. Rev. B* **51**, 13326 (1995).
- <sup>6</sup>D. M. Hofmann, D. Kovalev, G. Steude, B. K. Meyer, A. Hoffmann, L. Eckey, R. Heitz, T. Detchprom, H. Amano, and I. Akasaki, *Phys. Rev. B* **52**, 16702 (1995).
- <sup>7</sup>S. Fischer, C. Wetzels, E. E. Haller, and B. K. Meyer, *Appl. Phys. Lett.* **67**, 1298 (1995).
- <sup>8</sup>P. Perlin, T. Suski, H. Teisseyre, M. Leszczynski, I. Grzegory, J. Jun, S. Porowski, P. Boguslawski, J. Bernholc, J. C. Chervin, A. Polian, and T. D. Moustakas, *Phys. Rev. Lett.* **75**, 296 (1995).
- <sup>9</sup>T. Suski, P. Perlin, H. Teisseyre, M. Leszczynski, I. Grzegory, J. Jun, M. Bockowski, S. Porowski, and T. D. Moustakas, *Appl. Phys. Lett.* **67**, 2188 (1995).
- <sup>10</sup>A. Y. Polyakov, M. Shin, J. A. Freitas, M. Skowronski, D. W. Greve, and R. G. Wilson, *J. Appl. Phys.* **80**, 6349 (1996).
- <sup>11</sup>R. Zhang and T. F. Kuech, *Mater. Res. Soc. Symp. Proc.* **482**, 709 (1998).
- <sup>12</sup>R. Armitage, W. Hong, Y. Qing, H. Feick, J. Gebauer, E. R. Weber, S. Hautakangas, and K. Saarinen, *Appl. Phys. Lett.* **82**, 3457 (2003).
- <sup>13</sup>S. O. Kucheyev, M. Toth, M. R. Phillips, J. S. Williams, C. Jagadish, and G. Li, *J. Appl. Phys.* **91**, 5867 (2002).
- <sup>14</sup>V. Fiorentini, L. F. Bernardini, A. Bosin, and D. Vanderbilt, *Proceedings of the 23rd International Conference on the Physics of Semiconductors* (World Scientific, Singapore, 1996), Vol. 4, p. 2877.
- <sup>15</sup>J. Neugebauer and C. G. Van de Walle, *Appl. Phys. Lett.* **69**, 503 (1996).
- <sup>16</sup>H. Wang and A. B. Chen, *Phys. Rev. B* **63**, 125212 (2001).
- <sup>17</sup>A. F. Wright, *J. Appl. Phys.* **92**, 2575 (2002).
- <sup>18</sup>H. P. Maruska and J. J. Tietjen, *Appl. Phys. Lett.* **15**, 327 (1969).
- <sup>19</sup>J. Neugebauer and C. G. van de Walle, *Phys. Rev. B* **50**, 8067 (1994).
- <sup>20</sup>P. Boguslawski, E. Briggs, and J. Bernholc, *Proceedings of the 22nd International Conference on the Physics of Semiconductors* (World Scientific, Singapore, 1995), Vol. 3, p. 2331.

- <sup>21</sup>C. H. Seager, A. F. Wright, J. Yu, and W. Gotz, *J. Appl. Phys.* **92**, 6553 (2002).
- <sup>22</sup>D. D. Koleske, A. E. Wickenden, R. L. Henry, and M. E. Twigg, *J. Cryst. Growth* **242**, 55 (2002).
- <sup>23</sup>P. B. Klein, S. C. Binari, K. Ikossi, A. E. Wickenden, D. D. Koleske, and R. L. Henry, *Appl. Phys. Lett.* **79**, 3527 (2001).
- <sup>24</sup>C. R. Abernathy, J. D. MacKenzie, S. J. Pearton, and W. S. Hobson, *Appl. Phys. Lett.* **66**, 1969 (1995).
- <sup>25</sup>D. J. As and U. Kohler, *J. Phys.: Condens. Matter* **13**, 8923 (2001).
- <sup>26</sup>S. J. Pearton, C. R. Abernathy, and F. Ren, *Electron. Lett.* **30**, 527 (1994).
- <sup>27</sup>U. Birkle, M. Fehrer, V. Kirchner, S. Einfeldt, D. Hommel, S. Strauf, P. Michler, and J. Gutowski, *MRS Internet J. Nitride Semicond. Res.* **4S1**, (1999).
- <sup>28</sup>H. Tang, J. B. Webb, J. A. Bardwell, S. Raymond, J. Salzman, and C. Uzan-Saguy, *Appl. Phys. Lett.* **78**, 757 (2001).
- <sup>29</sup>M. E. Overberg, C. R. Abernathy, S. J. Pearton, R. G. Wilson, and J. M. Zavada, *Mater. Res. Soc. Symp. Proc.* **595**, W11.62.1-6 (1999).
- <sup>30</sup>S. Heikman, S. Keller, S. P. DenBaars, and U. K. Mishra, *Appl. Phys. Lett.* **81**, 439 (2002).
- <sup>31</sup>C. R. Elsass, T. Mates, B. Heying, C. Poblenz, P. Fini, P. M. Petroff, S. P. DenBaars, and J. S. Speck, *Appl. Phys. Lett.* **77**, 3167 (2000).